Effects of Temperature and Ionic Strength on the Rate and Equilibrium Constants for the Reaction $I^{\bullet}_{aq} + I^{-}_{aq} \leftrightarrow I_2^{\bullet-}{}_{aq}$

Yong Liu,[†] Ramona L. Sheaffer,[‡] and John R. Barker*[,†,§]

Department of Atmospheric, Oceanic, and Space Sciences, University of Michigan, Ann Arbor, Michigan 48109-2143, Department of Chemistry, University of Wyoming, Laramie, Wyoming 82071-3838, and Department of Chemistry, University of Michigan, Ann Arbor, Michigan 48109-1055

Received: July 21, 2003; In Final Form: September 22, 2003

Temperature-dependent forward (k_f) and reverse (k_r) constants for the title reaction were measured by analyzing the kinetics of formation and decay of $I_2^{\bullet-}$. Over the temperature range 286−320 K, the Arrhenius parameters are $k_f = (2.4 \pm 0.1) \times 10^{13} \exp[(-2324 \pm 77)/T]$ M^{-1} s^{-1} and $k_r = (2.6 \pm 0.4) \times 10^{12} \exp[(-5157 \pm 198)/T]$ s^{-1}. The equilibrium constant was found from the ratio of k_f/k_r: $K_{eq} = (9.2 \pm 1.4) \exp[(2833 \pm 212)/T]$ M^{-1}. Of particular interest, ionic strength effects on the rate constant of the title reaction are reported for the first time.

1. Introduction

The chemical reactions of iodine have been investigated extensively because radioactive and highly soluble cesium iodide is a major fission product.[1] The dissolved iodide may be either oxidized, yielding photochemically reactive species such as iodine (I_2) and hypoiodous acid (HOI), or methylated, yielding methyl iodide.[2,3]

More recently, halogen species have been implicated in the episodes of sudden, near-complete depletion of ozone observed in the polar marine boundary layer shortly after the spring equinox. Considerable effort has been directed toward understanding the conversion of the halide salts from sea salt aerosols to photochemically labile gas-phase halogen species.[4−8] Several oxidation−reduction chemical mechanisms and aqueous-phase free radical reactions have been proposed to explain "halogen activation",[9−13] in which dissolved halides are oxidized to produce photochemically labile halogen-containing compounds that can be photolyzed, hence initiating gas-phase chain reactions that destroy ozone. Although chloride is far more abundant than bromide or iodide in seawater,[10,14] the efficacy of the free radical mechanism that oxidizes the chloride[15] is inhibited by the high pH of seawater (pH ≈ 8[14]). The analogous mechanisms for oxidizing bromide and iodide are not affected by this range of pH values, and therefore, free radical mechanisms involving $Br_2^{\bullet-}$ and $I_2^{\bullet-}$ are more prevalent than that involving $Cl_2^{\bullet-}$, even though chloride is far more abundant.[14]

Dihalide radical anions have been studied for many years in biological and inorganic systems.[16−18] They are found to react according to the well-known reactions 1 and 2a,b to produce molecular halogens.[14,19]

$$X^{\bullet} + X^{-} \leftrightarrow X_2^{\bullet-} \quad (1)$$

$$X_2^{\bullet-} + X_2^{\bullet-} \rightarrow X_3^{-} + X^{-} \quad (2a)$$

$$X_3^{-} \rightarrow X_2 + X^{-} \quad (2b)$$

The molecular halogen may react further in solution, or it may escape into the gas phase, where it can be photolyzed. The equilibrium defined by reaction 1 is important because it regulates the relative concentrations of solvated $X^{\bullet}$ atoms, which are highly reactive, and $X_2^{\bullet-}$ radical anions, which are less reactive.[19] The equilibrium constants for X = Cl and Br at room temperature have been the subject of several investigations,[13,20−22] which are generally in good agreement. For X = I, however, the reported values of the equilibrium constant[1,23−27] range over a factor of 10 and the temperature dependence has only been reported twice prior to the present work.[1,24]

In the atmosphere, the ionic strength ranges from ∼10^{-5} M in cloudwater to ∼10 M in naturally dehydrated sea salt aerosols.[28] As a result, chemical reaction rate constants for aqueous-phase reactions involving ions can vary enormously in the atmosphere.[28] In many cases of interest, the reaction system is highly complex, hindering the direct investigation of ionic strength effects.[13] In contrast, the present reaction system with X = I is unusually simple, minimizing interference in direct measurements.

In this work, we have determined the forward and reverse rate constants of reaction 1 with X = I in the temperature range from 286 to 320 K, in the pH range from 1.1 to 10.8, and for ionic strengths ranging from 10^{-3} to ∼0.8 M. These conditions are found in the atmosphere and in relevant laboratory studies. The equilibrium constant was obtained as the ratio $K_{eq}(T) = k_f(T)/k_r(T)$, experimental errors were assessed, and all quantities were compared with values from the literature.

* To whom correspondence should be addressed. E-mail: jrbarker@umich.edu.
† Department of Atmospheric, Oceanic, and Space Sciences, University of Michigan.
‡ University of Wyoming.
§ Department of Chemistry, University of Michigan.

10.1021/jp036126a CCC: $25.00
Published on Web 11/11/2003

TABLE 1: Reactions Included in Simulations

reaction	k	ref	reaction	k	ref
$I^{\bullet} + I^{-} \rightarrow I_2^{\bullet-}$	8.9×10^9 M^{-1} s^{-1}	this work	$H^{\bullet} + I_2 \rightarrow H^+ + I_2^{\bullet-}$	3.5×10^{10} M^{-1} s^{-1}	36
$I_2^{\bullet-} \rightarrow I^{\bullet} + I^{-}$	6.5×10^4 s^{-1}	this work	$I^{\bullet} + I^{\bullet} \rightarrow I_2$	2.0×10^{10} M^{-1} s^{-1}	35
$I_2^{\bullet-} + I_2^{\bullet-} \rightarrow I_3^{-} + I^{-}$	2.3×10^9 M^{-1} s^{-1}	35	$I^{\bullet} + I_2^{\bullet-} \rightarrow I_3^{-}$	5.0×10^9 M^{-1} s^{-1}	35
$e^{-} + H^+ \rightarrow H^{\bullet}$	2.3×10^{10} M^{-1} s^{-1}	44	$O_2^{-} + H^+ \rightarrow HO_2^{\bullet}$	5.0×10^{10} M^{-1} s^{-1}	45
$e^{-} + O_2 \rightarrow O_2^{-}$	1.9×10^{10} M^{-1} s^{-1}	44	$HO_2^{\bullet} + I^{-} \rightarrow$ product	<100 M^{-1} s^{-1}	46
$e^{-} + I_2 \rightarrow I_2^{\bullet-}$	5.2×10^{10} M^{-1} s^{-1}	36	$HO_2^{\bullet} + I_2^{\bullet-} \rightarrow$ product	4.0×10^9 M^{-1} s^{-1}	3
$e^{-} + I_3^{-} \rightarrow I_2^{\bullet-} + I^{-}$	3.5×10^{10} M^{-1} s^{-1}	36	$HO_2^{\bullet} + I_2 \rightarrow H^+ + I_2^{\bullet-} + O_2$	1.8×10^7 M^{-1} s^{-1}	36
$H^{\bullet} + O_2 \rightarrow HO_2^{\bullet}$	2.0×10^{10} M^{-1} s^{-1}	36			

2. Experimental Section

The experimental approach consisted of excimer laser flash photolysis and time-resolved detection of transient species by multipass absorbance, as described elsewhere in detail.[22] All solutions were freshly prepared just before the experiments from the following reagents: NaI (Aldrich), >99%, certified; $HClO_4$ (Fisher), 70%, reagent ACS; $NaClO_4$ (Aldrich), >98%, certified. The water was purified by a Millipore MilliQ system, and the resistivity was >16 MΩ cm. Iodide ion concentrations were adjusted as desired in the range $(0.5-5) \times 10^{-5}$ M by adding weighed quantities of NaI. The acidity of the solutions was adjusted by adding perchloric acid ($HClO_4$).

For the ionic strength effect studies, sodium perchlorate ($NaClO_4$) was prepurified by filtration at an elevated temperature (~50 °C) to remove tiny suspended particles, which caused interference by scattering the laser light. When cooled to room temperature, the filtered solution became saturated, and solid sodium perchlorate precipitated. This saturated solution of sodium perchlorate was used as a stock reagent for preparing solutions for the ionic strength measurements. The concentration of the saturated stock solution was established by measuring its temperature and using the corresponding tabulated values of sodium perchlorate solubility.[29]

3. Results and Discussion

3.1. Chemical Mechanism and Data Analysis. A reasonably complete reaction mechanism is presented in Table 1. In the present experiments, iodine atoms were generated by the photodetachment of an electron from dissolved iodide ion[30] when irradiated by a 248 nm laser pulse:

$$I^{-} + h\nu \rightarrow I^{\bullet} + e^{-} \tag{3}$$

An immediate increase in the absorbance at 365 nm was observed after the laser pulse, followed by a slow decay back to the initial transmittance, as shown in Figure 1. The absorption was due to $I_2^{\bullet-}$ (absorption coefficient (base 10) of $\epsilon = 8800$ M^{-1} cm^{-1} at 365 nm[31]), which is produced by the following reaction mechanism:

$$I^{\bullet} + I^{-} \leftrightarrow I_2^{\bullet-} \tag{4}$$

$$I_2^{\bullet-} + I_2^{\bullet-} \rightarrow I_3^{-} + I^{-} \tag{5a}$$

$$I_3^{-} \leftrightarrow I_2 + I^{-} \tag{5b}$$

In computer simulations described below, it is shown that the other reactions in Table 1 and the absorption due to $I^{\bullet}$ and I_3^{-} can be neglected under the present experimental conditions. The time-dependent transmitted light intensity $I(t)$ depends on the absorbance $A(t)$ according to the Beer−Lambert equation:

$$I(t)/I_0 = 10^{-A(t)} = 10^{-\alpha s[I_2^{\bullet-}]} \tag{6}$$

where I_0 is the incident intensity of the probe light, s is the optical path length (~60 cm), α is the optical absorption coefficient at 365 nm, and the brackets denote concentration (mol L^{-1}).

To analyze the time-dependent transmitted light intensity, the chemical mechanism was used to derive an approximate analytical expression for the time-dependent $[I_2^{\bullet-}]$. The reaction mechanism is comprised of reactions 4, −4, and 5, resulting in the following coupled differential equations:

$$\frac{d[I_2^{\bullet-}]}{dt} = k_4[I^{\bullet}][I^{-}] - k_{-4}[I_2^{\bullet-}] - 2k_5[I_2^{\bullet-}]^2 \tag{7a}$$

$$\frac{d[I^{\bullet}]}{dt} = k_{-4}[I_2^{\bullet-}] - k_4[I^{\bullet}][I^{-}] \tag{7b}$$

The solution of these coupled equations is facilitated if the term that is second order in $[I_2^{\bullet-}]$ on the right-hand side of eq 7a can be neglected or treated as a first-order term. As in our previous work,[22] a first-order approximation was used to account approximately for the second-order term that appears in eq 7a:

$$2k_5[I_2^{\bullet-}]^2 \approx 2k_5[I_2^{\bullet-}]_{av}[I_2^{\bullet-}] = \gamma[I_2^{\bullet-}] \tag{8}$$

where $[I_2^{\bullet-}]_{av}$ is the average concentration and γ is a constant. As discussed previously,[22] this approximation is accurate when the extent of the loss of $I_2^{\bullet-}$ is small and the contribution from the second-order reaction is smaller than that from the first-order reactions, as is the case in the present experiments. Numerical simulations for the present experiments also support the accuracy of this approximation (see below). With this approximation, the coupled equations can be solved by using Laplace transforms, giving $[I_2^{\bullet-}]$ as a function of time:

$$[I_2^{\bullet-}] = k_4[I^{-}][I^{\bullet}]_0\frac{e^{-(k^I+\gamma)t} - e^{-\gamma t}}{k^I} = \frac{k_4[I^{-}][I^{\bullet}]_0}{k^I}\{1 - e^{-k^I t}\}e^{-\gamma t} \tag{9}$$

where $k^I = k_{-4} + k_4[I^{-}]$.

To analyze the experimental time-resolved absorbance data, the absorbance due to $I_2^{\bullet-}$ is described by eq 6 with $[I_2^{\bullet-}]$ described by eq 9. The constant γ is used merely as a fitting parameter, and no significance is placed on the values obtained for it. As can be seen in Figure 1, an intense pulse of scattered laser light contributes to the signals. This scattered light intensity is described accurately by an empirical exponential function, and the resulting expression for the transmitted monitoring light intensity consists of the sum of the Beer−Lambert expression and the empirical exponential term that describes the scattered light:[22]

$$I(t) = I_0 \times 10^{-\alpha s[I_2^{\bullet-}]} + I_{scat}e^{-t/\tau_{scat}} \tag{10}$$

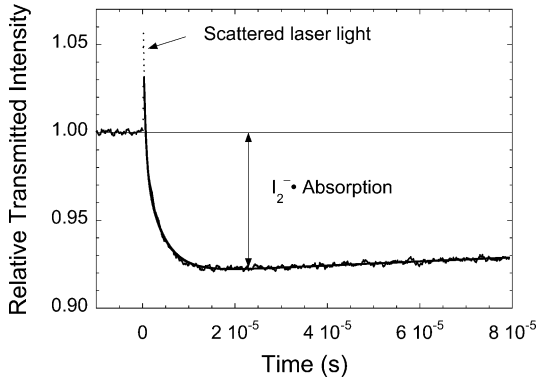

Figure 1. Typical time-dependent $I_2^{\bullet-}$ absorption data (points) and fitted curve (solid line) for $[I^-] = 2 \times 10^{-5}$ M.

where I_{scat} and τ_{scat} are the incident intensity and decay time constant, respectively, of the scattered laser light. The time-dependent light intensity at 365 nm (starting at $t = 1$ us) is fitted to eq 10 by nonlinear least squares carried out using KaleidaGraph (v. 3.5, Synergy Software), which utilizes the Marquardt−Levenberg algorithm.[32,33] Values for k^I obtained from the least-squares analysis are plotted as a function of $[I^-]$ to obtain the slope and intercept of the resulting straight line, which give k_4 and k_{-4}, respectively.

3.2. Numerical Simulations. To test the accuracy of the mechanism and of the approximation described by eq 8, numerical simulations were carried out for a mechanism consisting of reactions 4, −4, and 5, using a modified version of CHEMK,[34] which uses the Gear algorithm for numerical integration of stiff ordinary differential equations. Simulations were carried out using a range of $[I^\bullet]_0$ and $[I^-]$ typical of the experiments and the values for k_4 and k_{-4} found in the experiments. A literature value of rate constant $k_5 = 2.3 \times 10^9$ M^{-1} s^{-1} was used.[35] The resulting time-dependent $[I_2^{\bullet-}]$ values were used to generate sets of simulated experimental data that were then analyzed in the same manner as the actual experimental data. The analysis of the simulated data generally produced results in very good agreement with the rate constants used as input parameters in the simulations. The largest errors (on the order of a few percent) occur when $[I^-]$ is at the low end of its range, where reaction 4 is so slow that reaction 5 becomes more important, hence reducing the accuracy of the approximation in eq 8. The resulting *maximum* error in the extrapolated intercept (rate constant k_{-4}) of a plot of k^I vs $[I^-]$ is ≤5%; the slope is not affected significantly by the approximation. Since the temperature dependence of k_5 is not known, we assumed $k_5(T) = 0.33k_4(T)$ in simulations at all temperatures. The simulated results at temperatures throughout the range of the experiments show the errors for intercept and slope are not dependent on temperature.

In the present work, the hydrated electron (absorption coefficient[31] $\epsilon \approx 1300$ M^{-1} cm^{-1} at 365 nm) is not considered explicitly. Under typical experimental conditions (pH 3), electrons react quickly with H^+, producing H•, which initiates additional free radical reactions. To investigate the possible effects of the hydrated electron, simulations were conducted with the mechanism given in Table 1. The calculated $[I_2^{\bullet-}]$ and $[e^-]$ presented in Figure 2 show that the hydrated electron is consumed within less than 0.5 μs, and therefore does not affect the $I_2^{\bullet-}$ absorbance experimental data, which are fitted starting from $t = 1$ μs. Thus, any potential effect of the hydrated electron on the measured rate constants is negligible. In addition, the simulations show that I• and I_3^- can be neglected. As can be seen from Figure 2, $[I^\bullet]$ is up to 20 times as large as $[I_2^{\bullet-}]$, but

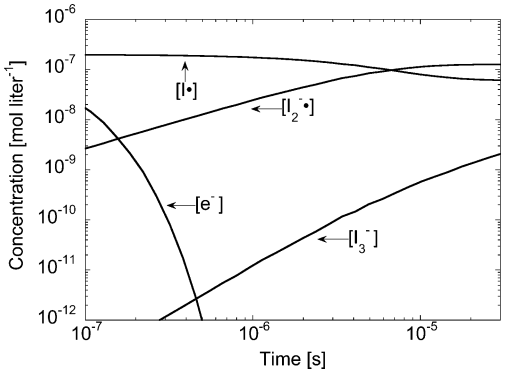

Figure 2. Concentration of dissolved electron and iodine-containing species as a function of time from numerical simulation (reactions in Table 1).

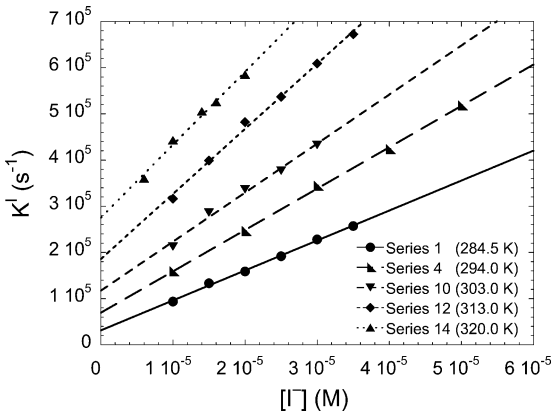

Figure 3. Pseudo-first-order rate constants (k^I) vs $[I^-]$ at various temperatures (see Table 2).

$[I_3^-]$ is at most 1/50 of $[I_2^{\bullet-}]$. The absorption coefficients of I• and I_3^- are $\epsilon(I^\bullet) \approx 50$ M^{-1} cm^{-1} at 365 nm (ref 31) and $\epsilon(I_3^-)_{max} = 2.58 \times 10^4$ M^{-1} cm^{-1} at 350 nm (ref 36), respectively. Given the calculated concentrations, the absorbances of I• and I_3^- are insignificant compared to that of $I_2^{\bullet-}$, and can be neglected. Analysis of simulated data with and without taking into account the I• and $I_3^{\bullet-}$ absorbance showed that the errors resulting from the neglect of the I• and $I_3^{\bullet-}$ absorbances are less than 1% at times greater than 1 μs after the laser pulse.

3.3. Determination of k_4, k_{-4}, and K_4. The experimental results are summarized in Table 2; typical results are shown in Figure 3. Each experiment series consists of at least five experiments with added iodide ion and at least one blank run containing just purified water. In all cases, k^I is a linear function of $[I^-]$ within experimental error, as expected from the mechanism. The slope and intercept are obtained by a linear least-squares analysis using equal weights (the experimental errors are essentially equal within each experiment series). From the expression for k^I, the slope and intercept correspond to rate constants k_4 and k_{-4}, respectively. The equilibrium constant is obtained from the ratio $K_4 = k_4/k_{-4}$. For each experiment series in Table 2 the uncertainties ($\pm\sigma$, 1 standard deviation) associated with k_4 and k_{-4} are measures of precision only, as obtained from the least-squares analysis; the uncertainties associated with K_4 are obtained by propagation of errors. The weighted averages of the values for k_4, k_{-4}, and K_4 at each temperature are given in Table 2. The results are presented as functions of $1/T$ in Figure 4. The activation energy and magnitude of k_4 indicate that it is diffusion controlled, similar to the analogous reaction for X = Br.[22]

3.4. Dissolved Oxygen and pH Dependence. Dissolved oxygen is not expected to influence the results,[22,37] and most

TABLE 2: Rate Constants and Equilibrium Constants[a]

series	T (K)	$k_4 \times 10^{-10}$ ($M^{-1}\,s^{-1}$)	$\pm\sigma_4 \times 10^{-10}$ ($M^{-1}\,s^{-1}$)	$k_{-4} \times 10^{-4}$ (s^{-1})	$\pm\sigma_{-4} \times 10^{-4}$ (s^{-1})	$K_4 \times 10^{-5}$ (M^{-1})	$\pm\sigma_{eq} \times 10^{-5}$ (M^{-1})
1	284.5	0.65	0.02	3.12	0.36	2.08	0.25
2	284.5	0.62	0.02	2.86	0.60	2.17	0.46
3	284.5	0.65	0.03	3.03	0.62	2.15	0.45
av	284.5	0.64	0.01	3.05	0.27	2.10	0.20
4	294.0	0.92	0.03	6.20	1.03	1.50	0.26
5	294.0	0.92	0.03	5.90	0.99	1.56	0.27
6	294.0	0.87	0.01	6.77	0.57	1.29	0.11
av	294.0	0.88	0.01	6.50	0.45	1.35	0.10
7	298.0	1.01	0.05	7.52	1.64	1.34	0.30
8	303.0	1.10	0.06	11.0	1.17	1.00	0.12
9	303.0	1.10	0.06	10.1	1.24	1.09	0.15
av	303.0	1.10	0.04	10.6	0.85	1.04	0.09
10	313.0	1.40	0.06	18.9	1.58	0.74	0.07
11	313.0	1.39	0.07	19.5	1.78	0.71	0.07
av	313.0	1.40	0.05	19.1	1.18	0.73	0.05
12	320.0	1.80	0.13	23.3	1.83	0.77	0.08
13	320.0	1.58	0.09	27.5	1.33	0.58	0.04
14	320.0	1.71	0.16	24.4	2.21	0.70	0.09
av	320.0	1.66	0.07	25.7	0.97	0.65	0.04
15[b]	294.0	0.89	0.05	6.44	1.23	1.38	0.28
16[c]	294.0	0.90	0.04	6.00	1.11	1.50	0.29
17[d]	293.0	0.89	0.03	7.00	1.12	1.27	0.20
18[e]	293.0	0.90	0.02	5.30	0.50	1.70	0.16
19[f]	293.0	0.92	0.01	5.30	0.54	1.74	0.12
20[g]	293.0	0.92	0.02	5.79	0.82	1.60	0.23
21[h]	293.0	0.95	0.01	5.50	0.49	1.75	0.16

[a] $\pm\sigma$ values are relative uncertainties (1 standard deviation). Except as noted, all solutions are at pH $\approx$ 3 and contained dissolved air. [b] Solution purged with helium. [c] Solution purged with oxygen. [d] pH 1.1. [e] pH 4.5. [f] pH 6.1. [g] pH 9.2. [h] pH 10.8.

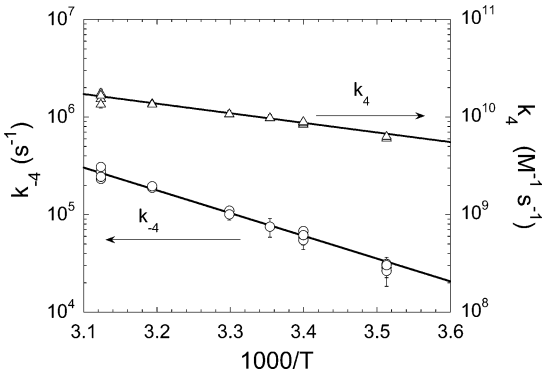

Figure 4. Forward (k_4) and reverse (k_{-4}) rate constants vs 1000/T (solid lines are nonlinear least-squares fits). Error bars ($\pm\sigma$) indicate precision only.

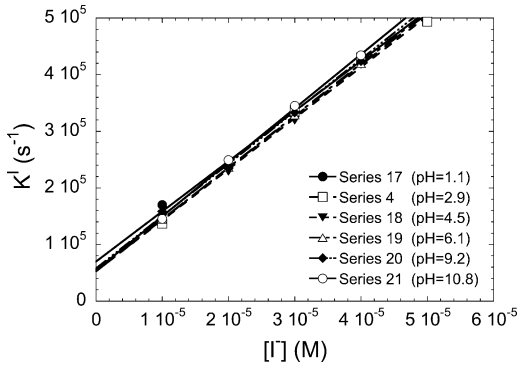

Figure 5. Pseudo-first-order rate constants (k^{I}) vs [I^-] at various conditions (see Table 2).

experiments were carried out using reagent solutions that are exposed to ambient air. The effect of dissolved oxygen was investigated by carrying out several series of experiments after the solutions were purged with high-purity helium or oxygen gas for 20 min. The results obtained with purged solutions (series 15 and 16; see Table 2) are indistinguishable from those obtained without purging.

The acidity of the solutions is not expected to influence the results, and most experiments were carried out at pH $\approx$ 3, where the pH is adjusted nominally by adding measured volumes of perchloric acid. However, to test for possible pH effects, experiments were conducted with pH ranging from 1.1 to 10.8 (measured using a pH meter equipped with a glass electrode, calibrated using appropriate buffer solutions). As can be seen from Table 2 and Figure 5, the experimental results with pH from 4.5 to 10.8 are indistinguishable from the experiments carried out at pH $\approx$ 3. The minor differences between series 4 (pH $\approx$ 3) and series 17 (pH 1.1) are probably due to the effect of the different ionic strengths. Ionic strength effects are discussed below.

3.5. Temperature Dependence. Arrhenius parameters were determined by carrying out a nonlinear least-squares analysis[32,38] using the average rate constants obtained at each temperature (Table 2). All of the rate constants are assumed to have equal weights. The results are shown as straight lines in Figure 4 and are given by eq 11,

$$k_4 = (2.37 \pm 0.59) \times 10^{13} \exp[-(2324 \pm 77)/T]\ M^{-1}\,s^{-1}, \quad \sigma^2_{AE} = 1.00 \times 10^{13}\ M^{-1}\,s^{-1}\,K \quad (11a)$$

$$k_{-4} = (2.58 \pm 1.62) \times 10^{12} \exp(-[5157 \pm 198)/T]\ s^{-1}, \quad \sigma^2_{AE} = 1.00 \times 10^{12}\ s^{-1}\,K \quad (11b)$$

where the standard deviations and covariances reflect the precision of the data. In these expressions, σ^2_{AE} is the covariance between the A factor and E_a/R (expressed in units of kelvin) in the Arrhenius equation [$k = A \exp(-E_a/RT)$], where E_a is the

activation energy and R is the gas law constant. Equilibrium constant K_4 is given by

$$K_4 = k_4/k_{-4} = (9.19 \pm 6.20) \exp[(2833 \pm 212)/T]\ \mathrm{M}^{-1} \quad (11c)$$

The preexponential factor and temperature dependence of K_4 give values for the entropy and enthalpy of reaction:

$$\Delta H_R^\circ = -23.6 \pm 1.8\ \mathrm{kJ\ mol}^{-1} \quad (12a)$$

$$\Delta S_R^\circ = 18.4 \pm 5.6\ \mathrm{J\ mol}^{-1}\ \mathrm{K}^{-1} \quad (12b)$$

The standard reduction potential $E^\circ(I_2^{\bullet -}/2I^-) = 1.03 \pm 0.01$ V is obtained from the equilibrium constant of reaction 4 (the present work) and the standard reduction potential vs NHE for $E^\circ(I^\bullet/I^-)$.[36] This value is in very good agreement with previously reported values.[36,39]

Prior to the present work, only two temperature-dependent measurements of the equilibrium constant had been reported.[1,24] The value for ΔH_R° found in the present experiments agrees with the literature values -23.5 and -22.9 ± 1.7 kJ mol^{-1} reported by Baxendale[24] and by Elliot and Sopchyshyn,[1] respectively. The equilibrium constants obtained in the present work at different temperatures are fairly consistent with corresponding values reported by Baxendale.[24] In contrast, our data differ from Elliot and Sopchyshyn's reported equilibrium constant[1] by about factor of 2 at room temperature. More recently, Elliot[35] reported a new value for the equilibrium constant at 293 K that is more than twice as large as the previous value and which is in good agreement with the present work.

3.6. Results and Error Discussion: Low Ionic Strength. Systematic errors in this work can arise from several sources. These include the approximations used in the derivation of eq 9, the effect of temperature differences in the cell, and possible concentration variations from solution preparation. As described above, numerical tests of the approximations used in derivation of eq 9 showed the k_{-4} was affected by a maximum of 5%, while k_4 was hardly affected at all. This maximum 5% error will also affect the equilibrium constant K_4. Thus, we assume that the approximations used in this analysis have no effect on k_4, but affect both k_{-4} and K_4 by 5%. In most experiments, the measured temperature differences between the entrance and exit of the cell were less than 0.5 °C. However, the differences were sometimes as large as 1 °C at the ends of the temperature range. According to the Arrhenius parameters given below, a temperature difference of 1 K causes variations of 2.6%, 5.8%, and about 3.2% in k_4, k_{-4}, and K_4, respectively. The errors that arise from solution preparation are estimated to be less than 1%.

Taking into account all systematic and random errors, we conclude that k_4, k_{-4}, and K_4 may be affected by up to ~5%, 15%, and ~15% (1 standard deviation) at temperatures in the range of the experiments (286−320 K). Computer simulations with the mechanism in Table 1 showed that the errors are not temperature dependent, and we conclude it is reasonable to assume the systematic errors are associated with the preexponential factor. Thus, the rate constants and equilibrium constant are expressed as eq 13.

$$k_4 = (2.37 \pm 0.12) \times 10^{13} \exp[-(2324 \pm 77)/T]\ \mathrm{M}^{-1}\ \mathrm{s}^{-1} \quad (13a)$$

$$k_{-4} = (2.58 \pm 0.39) \times 10^{12} \exp[-(5157 \pm 198)/T]\ \mathrm{s}^{-1} \quad (13b)$$

$$K_4 = (9.19 \pm 1.38) \exp[(2833 \pm 212)/T]\ \mathrm{M}^{-1} \quad (13c)$$

TABLE 3: Comparisons of Rate Constants and Equilibrium Constants[a]

$k_4 \times 10^{-10}$ (M^{-1} s^{-1})	$k_{-4} \times 10^{-4}$ (s^{-1})	$K_4 \times 10^{-5}$ (M^{-1})	T (K)	ref
0.76		1.13	294	23
		1.13	294	24
		0.84		25
0.98	90	0.11	293	26
2	170	0.12		27
		0.50	294	1
1.1				30
1.2		1.1 ± 15%	298	36
1.1		1.13		47
1.1 ± 0.5			295 ± 2	3
0.88		1.28	293	35
0.88 ± 0.01	6.50 ± 0.45	1.35 ± 0.10	294	this work

[a] Uncertainties stated as in the original papers.

The present rate constant results are compared with those from previous investigations in Table 3, where it is apparent that the present results are consistent with most previous results, considering the temperature differences and stated experimental uncertainties. Although the rate constants and equilibrium constant have been studied previously in several investigations at room temperature,[1,23−27] only two previous temperature-dependent measurements have been reported.[1,24] The forward reaction 1 with X = I is at the diffusion-controlled limit, as are the analogous reactions with X = Br and Cl.[13,22] The forward rate constants of reaction 1 for Cl, Br, and I are 7.8×10^9 s^{-1} (ref 13), 1.2×10^{10} s^{-1} (ref 22), and 8.8×10^9 s^{-1} (present work), respectively. Explanations for the minor differences among these rate constants are not apparent.

3.7. Ionic Strength Dependence. The ionic strength is important in concentrated solutions because each ion is surrounded by an extended solvation shell that can affect ionic activities and reaction rate constants. The ionic strength influence on the reaction rate constants k_4 and k_{-4} had not been investigated previously. In this work, experiments were carried out at $NaClO_4$ concentrations up to 1.0 M. The filtration of the $NaClO_4$ solutions, as described in the Experimental Section, reduced the effects of scattered laser light at ionic strengths less than 1 M, but at higher concentrations the scattered light interference became intolerable.

Transition-state theory has been combined with the Debye−Hückel (DH) theory and an empirical term $f(\mu)$ introduced by Davies to obtain the Debye−Hückel−Brønsted−Davies (DHBD) equation:[40]

$$\log k = \log k^\circ + 2Z_A Z_B A \left\{ \frac{\mu^{1/2}}{1 + \mu^{1/2}} \right\} - f(\mu) \quad (14)$$

where k is the observed rate constant, k° is the rate constant at infinite dilution, A is the Debye−Hückel constant ($A = 0.509$ at 298 K), Z_A and Z_B are charges for species A and B, respectively, μ is the total ionic strength, and $f(\mu)$ is an empirical term, usually expressed as a power series. Because the increased ionic atmosphere at higher ionic strength screens the electrostatic interaction between species A and B, the effect of the ionic strength is to increase the rate constant for ions with charges of the same sign and to decrease it when the charges are opposite in sign, as predicted by eq 14. The activity coefficient of an ion does not monotonically approach zero as the ionic strength increases, but it can increase again for large μ because the amount of solvent available for solvation of ions decreases as μ increases; decreasing the amount of water tends to reduce solvation screening, and ions become more active once again.[41]

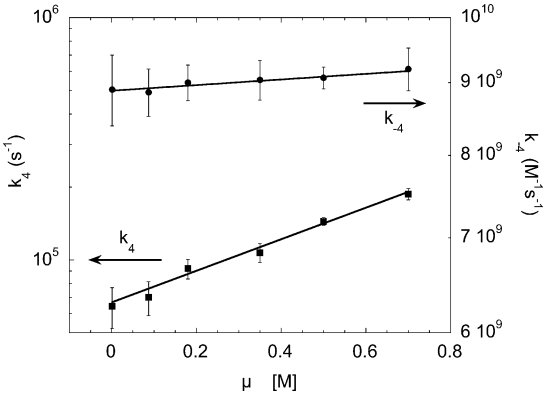

Figure 6. Ionic strength dependence of forward (k_4) and reverse (k_{-4}) rate constants (solid lines are nonlinear least-squares fits). Error bars ($\pm\sigma$) indicate precision only.

In the present system, $I^{\bullet}$ is neutral, and thus, rate constant k_4 depends only on the empirical term $f(\mu)$ in eq 14. The Debye−Hückel equation does not apply to unimolecular reactions, and thus, any ionic strength dependence of k_{-4} will consist of empirical terms. At higher ion concentrations, $f(\mu)$ is expressed as a power series, but usually only the linear term with coefficient b is retained:

$$\log k = \log k^{\circ} + b\mu \tag{15}$$

The empirical constant b depends on the difference between the activities of the reactants and the transition state, and even its sign cannot be predicted with certainty.[42] Figure 6 presents the data for k_4 and k_{-4} as functions of μ. It is clear that both k_4 and k_{-4} increase with increasing ionic strength, and they can be fitted by eq 15. Note that $NaClO_4$ does not dissociate completely and there exists an equilibrium and corresponding equilibrium constant:[43]

$$NaClO_4 \leftrightarrow Na^+ + ClO_4^- \ (K_{eq} = 0.2\ M^{-1}) \tag{16}$$

This equilibrium was used in calculating the ionic strength.

A nonlinear least-squares analysis of the results according to eq 15 gives the following expressions for the rate constants at 294 K:

$$k_4 = (8.89 \pm 0.02) \times 10^9 \exp[(0.04 \pm 0.04)\mu], \quad \sigma^2_{kb} = 0.22 \times 10^9\ M^{-2}\ s^{-1} \tag{17a}$$

$$k_{-4} = (6.97 \pm 0.52) \times 10^4 \exp[(1.18 \pm 0.12)\mu], \quad \sigma^2_{kb} = 0.52 \times 10^4\ M^{-1}\ s^{-1} \tag{17b}$$

$$K_4 = (1.28 \pm 0.10) \times 10^5 \exp[(-1.14 \pm 0.13)\mu] \tag{17c}$$

where the uncertainties correspond to 1σ standard deviations and σ^2_{kb} is the covariance between k° and b. It is seen that k_4 has a very weak dependence on the ionic strength, probably because the reaction is at the diffusion-controlled limit. By analogy, we anticipate that the rate constants of reaction 1 with X = Cl and Br may also be only weakly dependent on ionic strength.

Liquid water is universally present in the atmospheric condensed phase, and the ionic strength ranges over several orders of magnitude. Hence, although the effect is often neglected in atmospheric chemical models, we expect that many aqueous-phase reaction rate constants are strongly influenced by ionic strength.

Acknowledgment. Y.L. and J.R.B. thank the Atmospheric Chemistry Division of NSF for financial support. R.L.S. thanks the Research Experience for Undergraduates Program funded by NSF (Grant NSF-CHE0097585, in the Chemistry Department, University of Michigan) for support. We all thank Beth Percha and Amran Gowani for assistance with some of the experiments. We also thank a reviewer who called our attention to the dissociation constant for $NaClO_4$. (This material is based upon work supported by the National Science Foundation under Grant No. 9812680.)

References and Notes

(1) Elliot, A. J.; Sopchyshyn, F. C. *Int. J. Chem. Kinet.* **1984**, *16*, 1247−56.
(2) Lovelock, J. E.; Maggs, R. J.; Wade, R. J. *Nature* **1973**, *241*, 194−96.
(3) Ishigure, K.; Shiraishi, H.; Okuda, H. *Radiat. Phys. Chem.* **1988**, *32*, 593−97.
(4) Barrie, L. A.; Bottenheim, J. W.; Schnell, R. C.; Crutzen, P. J.; Rasmussen, R. A. *Nature* **1988**, *334*, 138−41.
(5) Bottenheim, J. W.; Barrie, L. A.; Atlas, E.; Heidt, L. E.; Niki, H.; Rasmussen, R. A.; Shepson, P. B. *J. Geophys. Res.* **1990**, *95*, 18555−68.
(6) McConnell, J. C.; Henderson, G. S.; Barrie, L.; Bottenheim, J.; Niki, H.; Langford, C. H.; Templeton, E. M. J. *Nature* **1992**, *355*, 150−52.
(7) Von Glasow, R.; Sander, R.; Bott, A.; Crutzen, P. J. *J. Geophys. Res.* **2002**, *107* (D17), 4341.
(8) Platt, U.; Honninger, G. *Chemosphere* **2003**, *52*, 325−38.
(9) Sander, R.; Crutzen, P. J. *J. Geophys. Res.* **1996**, *101*, 9121−38.
(10) Finlayson-Pitts, B. J.; Hemminger, J. C. *J. Phys. Chem. A* **2000**, *104*, 11463−77.
(11) Foster, K. L.; Plastridge, R. A.; Bottenheim, J. W.; Shepson, P. B.; Finlayson-Pitts, B. J.; Spicer, C. W. *Science* **2001**, *291*, 471−4.
(12) Yu, X.-Y. Kinetics of Free Radical Reactions Generated by Laser Flash Photolysis of $OH+Cl^-$ and $SO_4^-+Cl^-$ in the Aqueous Phase—Chemical Mechanism, Kinetics Data and Their Implications. Ph.D. (Chemistry), University of Michigan, 2001.
(13) Yu, X.-Y.; Bao, Z.-C.; Barker, J. R. *J. Phys. Chem. A.*, submitted for publication.
(14) Finlayson-Pitts, B. J.; Pitts, J. N., Jr. *Chemistry of the Upper and Lower Atmosphere*; Academic Press: San Diego, 2000.
(15) Yu, X.-Y.; Barker, J. R. *J. Phys. Chem. A* **2003**, *107*, 1313−24.
(16) Adams, G. E.; Aldrich, J. E.; Bisby, R. H.; Cundall, R. B.; Redpath, J. L.; Willson, R. L. *Radiat. Res.* **1972**, *49*, 278.
(17) Adams, G. E.; Bisby, R. H.; Cundall, R. B.; Redpath, J. L.; Willson, R. L. *Radiat. Res.* **1972**, *49*, 290.
(18) Prutz, W. A.; Butler, J.; Land, E. J. *Int. J. Radiat. Biol. Relat. Stud. Phys. Chem. Med.* **1985**, *47*, 149.
(19) Huie, R. E. Free radical chemistry of the atmospheric aqueous phase. In *Progress and Problems in Atmospheric Chemistry*, 1st ed.; Barker, J. R., Ed.; World Scientific: Singapore, 1995; pp 374−419.
(20) Adams, D. J.; Barlow, S.; Buxton, G. V.; Malone, T. N.; Salmon, G. A. *J. Chem. Soc., Faraday Trans. 1* **1995**, *91*, 3303−5.
(21) Buxton, G. V.; Bydder, M.; Salmon, G. A. *J. Chem. Soc., Faraday Trans. 1* **1998**, *94*, 653−7.
(22) Liu, Y.; Pimentel, A. S.; Antoku, Y.; Giles, B. J.; Barker, J. R. *J. Phys. Chem. A* **2002**, *106*, 11075−82.
(23) Baxendale, J. H.; Bevan, P. L. T.; Stott, D. A. *Trans. Faraday Soc.* **1968**, *64*, 238−97.
(24) Baxendale, J. H.; Bevan, P. L. T. *J. Chem. Soc. A* **1969**, 2240.
(25) Thomas, J. K. *Adv. Radiat. Chem.* **1969**, *1*, 103.
(26) Barkatt, A.; Ottolenghi, M. *Mol. Photochem.* **1974**, *6*, 253−61.
(27) Fornier de Violet, P.; Bonneau, R.; Logan, S. R. *J. Phys. Chem.* **1974**, *78*, 1698−701.
(28) Seinfeld, J. H.; Pandis, S. N. *Atmospheric Chemistry and Physics*; John Wiley & Sons: New York, 1998.
(29) Aqueous solubility of inorganic compounds at various temperatures. In *CRC Handbook of Chemistry and Physics*, 81st ed.; Lide, D. R., Ed.; CRC Press: Boca Raton, FL, 2000; p 8.102.
(30) Nagarajan, V.; Fessenden, R. W. *J. Phys. Chem.* **1985**, *89*, 2330−35.
(31) Hug, G. L. *Optical Spectra of Nonmetallic Inorganic Transient Species in Aqueous Solution*; National Bureau of Standards, U.S. Department of Commerce: Washington, DC, 1981; Vol. 69.
(32) Marquardt, D. W. *J. Soc. Ind. Appl. Math.* **1963**, *11*, 431.
(33) Bevington, P. R. *Data Reduction and Error Analysis for the Physical Sciences*; McGraw-Hill: New York, 1969.
(34) Whitten, G. Z.; Hogo, H. *CHEMK*; Science Applications Inc.: San Rafael, CA, 1980.
(35) Elliot, A. J. *Can. J. Chem.* **1992**, *70*, 1658.

(36) Schwarz, H. A.; Bielski, B. H. J. *J. Phys. Chem.* **1986**, *90*, 1445−48.
(37) Treinin, A.; Hayon, E. *J. Am. Chem. Soc.* **1975**, *97*, 1716−21.
(38) Synergy. *KaleidaGraph*, 3.51 ed.; Synergy Software: Reading, PA, 2001.
(39) Stanbury, D. M.; Wilmarth, W. K.; Khalaf, S.; Po, H. N.; Byde, J. E. *Inorg. Chem.* **1980**, *19*, 2715−22.
(40) Perlmutter-Hayman, B. *Prog. React. Kinet.* **1971**, *6*, 239−67.
(41) Bockris, J. O. M.; Reddy, A. K. N. *Modern Electrochemistry*; Plenum: New York, 1970; Vol. 1.
(42) Moore, J. W.; Pearson, R. G. *Kinetics and Mechanism*, 3rd ed.; John Wiley & Sons: New York, 1981.
(43) Hogfeldt, E. *Stability constants of metal-ion complexes, Part A: Inorganic Ligands*, 21st ed.; Pergamon Press: New York, 1982.
(44) Buxton, G. V.; Greenstock, C. L.; Helman, W. P.; Ross, A. B. *J. Phys. Chem. Ref. Data* **1988**, *17*, 513−886.
(45) Ilan, Y.; Rabani, J. *Int. J. Radiat. Phys. Chem.* **1976**, *8*, 609−11.
(46) Hart, E. J.; Henglein, A. *J. Phys. Chem.* **1985**, *89*, 4342−47.
(47) Ishigure, K.; Shiraishi, H.; Okuda, H.; Fujita, N. *Radiat. Phys. Chem.* **1986**, *28*, 601−10.